

Open access • Journal Article • DOI:10.1016/J.DSR2.2018.07.001

Temporal variability of downward fluxes of organic carbon off Monterey Bay — Source link [2]

Carmen G. Castro, Francisco P. Chavez, J. Timothy Pennington, Reginaldo Durazo ...+1 more authors

Institutions: Spanish National Research Council, Monterey Bay Aquarium Research Institute, Autonomous University of Baja California, Naval Postgraduate School

Published on: 01 May 2018 - Deep-sea Research Part li-topical Studies in Oceanography (Pergamon)

Topics: Monterey Canyon, Sediment trap, Upwelling and Bay

Related papers:

- Downward fluxes of sinking particulate matter in the deep Ionian Sea (NESTOR site), eastern Mediterranean: seasonal and interannual variability
- Dynamics of particle flux and carbon export in the northwestern Mediterranean Sea: A two decade time-series study at the DYFAMED site
- Temporal methane variability in the water column of an area of seasonal coastal upwelling: A study based on a 12 year time series
- Vertical and temporal variations of particle fluxes in the deep tropical atlantic
- Particle fluxes at the Australian Southern Ocean Time Series (SOTS) achieve organic carbon sequestration at rates close to the global median, are dominated by biogenic carbonates, and show no temporal trends over 20-years

Share this paper: 🚯 🎽 🛅 🗠

1	Temporal variability of downward fluxes of organic carbon off
2	Monterey Bay
3	
4	
5	Carmen G. Castro ^{a,*} , Francisco P. Chavez ^b , J. Timothy Pennington ^b , Reginaldo Durazo ^c
6	and Curtis A. Collins ^d
7	
8 9	a Conscio Superior de Investigaciones Científicas Institute de Investigaciones Marinas E
9 10	^a Consejo Superior de Investigaciones Científicas, Instituto de Investigaciones Marinas, E- 36208, Vigo, Spain
11	^b Monterey Bay Aquarium Research Institute, Moss Landing, CA 95039 USA
12	° Facultad de Ciencias Marinas, Universidad Autónoma de Baja California, Ensenada, Baja
13	California, México
14	^d Department of Oceanography, Naval Postgraduate School, Monterey, CA 93943
15	
16	
17	*Corresponding author.
18	E-mail address: cgcastro@iim.csic.es (C.G. Castro)
19	
17	
20	Key words: Vertical fluxes; Organic carbon; Coastal upwelling; Monterey Bay, California
21	Current System, Annual variability, 36.6°N, 122.4°W
21	Current System, Annual Variability, 50.0 TV, 122.4 VV
22	Running head: Downward fluxes of organic carbon
23	Color: Figures 1, 8 and 10 to be printed in color

- 26 ABSTRACT
- 27

28 Sediment traps were deployed at two depths (300 m and 1200 m) off Monterey Bay (36°40'N and 122°25'W, Central California) for 7.3 years (1998 – 2005). The sediment trap data provided 29 30 information about the quantity and quality of settling material, and allowed exploration of the relationship of the sinking material with the environmental conditions in this coastal upwelling 31 32 region. The magnitude and composition of the settling material were highly variable over time. Organic carbon (Corg) fluxes ranged between 4 - 296 mgC·m⁻²·day⁻¹ and 0.1 - 142 mgC·m⁻²·day⁻¹ 33 for shallow and deep sediment traps, respectively. The time series of Corg vertical flux was 34 characterized by pulses of intense fluxes that were associated with peaks of primary production, 35 36 generally during upwelling periods. Despite considerable variability, fluxes varied seasonally with highest values during the upwelling season and the lowest in winter. Attenuation of Corg 37 vertical fluxes with depth (300 m vs. 1200 m) varied between 31% and 24% except for the late 38 39 upwelling period, when there was an increase with depth likely due to resuspension of material 40 from Monterey Canyon. Calculation of a seasonal vertical budget of organic carbon off 41 Monterey Bay resulted in a transfer between 4.0% and 4.9% of the primary production to the 42 deep ocean, suggesting that coastal upwelling efficiently sequestered CO₂.

43

44

- 46 1. Introduction
- 47

48 The biological pump, including all processes through which photosynthetically produced organic matter is transported from surface waters to the deep ocean (Volk and Hoffert, 1985), 49 50 plays an important role in the global ocean carbon cycle. The biological pump is the main 51 mechanism for removing CO_2 from the atmosphere and sequestering it in the deep sea (Gruber 52 and Sarmiento, 2002; Passow and Carlson, 2012). The rate that the biological pump sequesters 53 CO_2 is of key importance for the Earth's climate regulation (Sigman and Boyle, 2000; Riebesell 54 et al., 2009; IPCC 2013). 55 Carbon fixed by primary production is transferred to the deep ocean principally by (1) 56 passively sinking particles, (2) vertical mixing of dissolved organic matter and (3) active 57 transport by animals (Ducklow et al., 2001; Turner, 2015). Sinking particles constitute the main 58 vector of downward transport of carbon (Sigman and Boyle, 2000; Buesseler et al., 2007), 59 accounting for up to 80% of the carbon reaching the deep sea (Hansell, 2002; Hopkinson and 60 Vallino, 2005). While sinking through the water column, there is a substantial attenuation of the particulate organic carbon (Corg) flux with the majority of the sinking Corg lost between 100 m 61 62 and 500 m (Martin et al., 1987) due to remineralization (which converts it back to dissolved 63 carbon dioxide) and solubilization processes (Martin et al., 1987; Steinberg et al., 2008). There 64 is large variability in export of organic matter from the euphotic zone (export flux). The export 65 flux averages 30% of net primary production in polar regions but is much lower, <10% of net 66 primary production, at low latitudes (Antia et al., 2001; Henson et al., 2011). Following De La 67 Rocha and Passow (2007), the efficiency of the biological pump is here taken as the proportion 68 of export flux that reaches the base of the mesopelagic zone (~ 1000 m). Sinking material that

69 reaches this depth is effectively removed from interaction with the atmosphere for more than

70 100 years (Lampitt et al., 2008) and is considered 'sequestered'. This sequestration flux

71

Abbreviations: C_{org}, particulate organic carbon; C_{inorg}, particulate inorganic carbon; N, nitrogen;
 EU, early upwelling, February to April; LU, late upwelling, May to July; OC, oceanic, August
 to October; DV, Davidson, November to January; RCM, recording current meter; ADCP,

75 acoustic Doppler current profiler; IRS, indented rotated sphere

typically constitutes 6-25% of net primary production (Honda et al., 2002; Passow and Carlson,2012).

79 Continental margins play a key role in the cycling of organic matter (Walsh, 1991; 80 Falkowski et al., 1988; Liu et al., 2010; Bauer et al., 2013). Despite covering <15% of the total 81 ocean surface, about 27% to 30% of ocean CO_2 uptake from the atmosphere occurs within the 82 continental margins (Chen and Borges, 2009). Some portion of this carbon uptake at the 83 continental margin is ultimately exported to the deep sea or buried in margin sediments via the 84 coastal (biological and solubility) pump. On the other hand, combining satellite annual global 85 net primary production estimates with an empirical model of Corg sequestration, Muller-Karger 86 et al. (2005) calculated that much more carbon sequestration takes places at continental margins 87 (>40%). These large uncertainties remain due to the variety of food webs and biogeochemical 88 transformations inherent to these coastal marine ecosystems (Inthorn et al., 2006; Liu et al., 89 2010).

90 Among margins, coastal upwelling regions constitute an extreme case as they are among the 91 most productive marine ecosystems in the world. Despite covering <1% of the global ocean 92 surface, they support about 5% of global marine primary production (Carr, 2003) and thus play 93 a significant role in the biological pump on a global scale. Central California is one of these 94 coastal upwelling regions, with prevailing northwesterly wind driven upwelling through spring 95 and summer and favoring high primary production levels (Pennington and Chavez, 2000; 96 Chavez et al., 2011). Pilskaln et al. (1996) assessed the fate of the organic carbon fixed in 97 Monterey Bay (Central California) based on a 3-year time series of sediment trap data at 450 m 98 and using previous measurements of benthic fluxes to indirectly calculate the organic carbon 99 flux at the base of the mesopelagic. They estimated that on an annual basis, 1.6% of this 100 production reached the seafloor while 81% of the net primary production was exported offshore 101 by Ekman transport.

In this manuscript, the vertical flux of organic matter collected by sediment traps at 300 m
and 1200 m depth in the coastal upwelling zone off Central California, from February 1998 to
July 2005, were analyzed. Our goals are to (1) determine the seasonal and interannual variability

105	of vertical flux of organic carbon, (2) estimate seasonal organic carbon budgets and (3) discuss
106	the efficiency of coastal upwelling in sequestering CO_2 on the basis of particulate organic matter
107	fluxes.
108	
109	
110 111	2. Material and methods
112 113 114	2.1. Study site
115	Monterey Bay, located in Central California, is a large open bay bisected by the Monterey
116	Submarine Canyon, which runs east to west through the middle of the Bay (Fig. 1). Off Central
117	California, hydrodynamic and biogeochemical variability is largely controlled by northwesterly
118	winds that are in part responsible for the California Current and generate coastal upwelling
119	(Strub et al., 1987; Pennington and Chavez, 2000, Collins et al., 2003). Based on thermohaline
120	and biogeochemical properties for the coastal zone, inshore of the California Current,
121	Pennington and Chavez (2000) defined four seasonal periods (1) spring (early) and (2) summer
122	(late) upwelling seasons, from February to April and from May to July, respectively; (3) a fall
123	(oceanic) season from August to October and (4) a winter (Davidson) period from November to
124	the following January. Surface waters are cold and salty during early upwelling (EU) and warm
125	during late upwelling (LU), remain warm but freshen in the oceanic (OC) season and cool again
126	for the Davidson (DV) season. The EU and LU seasons exhibit the highest surface nutrients and
127	primary production, mainly due to diatom blooms. During these seasons, the biologically
128	productive waters extend several hundred kilometers from shore, to the inshore edge of the
129	California Current (Collins et al., 2003). Phytoplankton blooms, primarily composed of oceanic
130	picoplankton, continue to develop intermittently for the OC season. In fact, during this season
131	there is an onshore shift of the California Current, about 80 km toward shore. During the DV
132	season, primary production is low, regulated by low levels of nitrate, light and temperature.
133	

2.2. Sample collection 2.2.1. Cruises

136 137	Station M2, near the mouth of Monterey Bay (Fig. 1), has been occupied bimonthly				
138	since 1993 as part of the Monterey Bay Time Series (Chavez et al., 2002). In this study,				
139	observations took place between 1998 and 2006. Methods used to collect hydrographic data				
140	were given by Asanuma et al. (1999). Methods for biological and chemical measurements have				
141	been described by Pennington and Chavez (2000). Briefly, a SeaBird 911 CTD was used for				
142	collecting the hydrographic data to at least 200 m and Niskin bottle samples for nutrients,				
143	chlorophyll a and primary production were obtained from the sea surface to 200 m during each				
144	cast. Nutrient samples were frozen unfiltered aboard ship and later processed on an AlpChem				
145	autoanalyzer (Sakmato et al., 1990). Primary production (PP) was measured by ¹⁴ C uptake in 24				
146	h in situ incubations (Pennington and Chavez, 2000). Water column-integrated PP was				
147	calculated by using trapezoidal integrations of PP over the euphotic zone.				
148					
149	2.2.2. Mooring deployment				
150					
150 151	From 1998 to 2006, a mooring designated S2, was deployed on the continental slope				
	From 1998 to 2006, a mooring designated S2, was deployed on the continental slope near M2 at 36°40'N and 122°25'W and 1800 m depth (Fig. 1). The mooring included an				
151					
151 152	near M2 at 36°40'N and 122°25'W and 1800 m depth (Fig. 1). The mooring included an				
151 152 153	near M2 at 36°40'N and 122°25'W and 1800 m depth (Fig. 1). The mooring included an upward looking 300 kHz RD Instruments ADCP at 300 m depth, two current meters at 305 m				
151 152 153 154	near M2 at 36°40'N and 122°25'W and 1800 m depth (Fig. 1). The mooring included an upward looking 300 kHz RD Instruments ADCP at 300 m depth, two current meters at 305 m and 1200 m depth and two sediment traps just below each current meter. Deployments lasted for				
151 152 153 154 155	near M2 at 36°40'N and 122°25'W and 1800 m depth (Fig. 1). The mooring included an upward looking 300 kHz RD Instruments ADCP at 300 m depth, two current meters at 305 m and 1200 m depth and two sediment traps just below each current meter. Deployments lasted for five to six months except the last deployment which was for 10 months (Table 1). In the				
151 152 153 154 155 156	near M2 at 36°40'N and 122°25'W and 1800 m depth (Fig. 1). The mooring included an upward looking 300 kHz RD Instruments ADCP at 300 m depth, two current meters at 305 m and 1200 m depth and two sediment traps just below each current meter. Deployments lasted for five to six months except the last deployment which was for 10 months (Table 1). In the following sections, measurements at the upper (lower) level will be referred to as "300 m"				
151 152 153 154 155 156 157	near M2 at 36°40'N and 122°25'W and 1800 m depth (Fig. 1). The mooring included an upward looking 300 kHz RD Instruments ADCP at 300 m depth, two current meters at 305 m and 1200 m depth and two sediment traps just below each current meter. Deployments lasted for five to six months except the last deployment which was for 10 months (Table 1). In the following sections, measurements at the upper (lower) level will be referred to as "300 m" ("1200 m") nominal depth.				
151 152 153 154 155 156 157 158	near M2 at 36°40'N and 122°25'W and 1800 m depth (Fig. 1). The mooring included an upward looking 300 kHz RD Instruments ADCP at 300 m depth, two current meters at 305 m and 1200 m depth and two sediment traps just below each current meter. Deployments lasted for five to six months except the last deployment which was for 10 months (Table 1). In the following sections, measurements at the upper (lower) level will be referred to as "300 m" ("1200 m") nominal depth. Aanderaa recording current meters (RCM8) were used. Current speed was measured by				
151 152 153 154 155 156 157 158 159	near M2 at 36°40'N and 122°25'W and 1800 m depth (Fig. 1). The mooring included an upward looking 300 kHz RD Instruments ADCP at 300 m depth, two current meters at 305 m and 1200 m depth and two sediment traps just below each current meter. Deployments lasted for five to six months except the last deployment which was for 10 months (Table 1). In the following sections, measurements at the upper (lower) level will be referred to as "300 m" ("1200 m") nominal depth. Aanderaa recording current meters (RCM8) were used. Current speed was measured by rotations of a shrouded paddle-type rotor which was magnetically linked to an electronic				
151 152 153 154 155 156 157 158 159 160	near M2 at 36°40'N and 122°25'W and 1800 m depth (Fig. 1). The mooring included an upward looking 300 kHz RD Instruments ADCP at 300 m depth, two current meters at 305 m and 1200 m depth and two sediment traps just below each current meter. Deployments lasted for five to six months except the last deployment which was for 10 months (Table 1). In the following sections, measurements at the upper (lower) level will be referred to as "300 m" ("1200 m") nominal depth. Aanderaa recording current meters (RCM8) were used. Current speed was measured by rotations of a shrouded paddle-type rotor which was magnetically linked to an electronic counter and current direction was measured by magnetic compass. Before deployment, the				
151 152 153 154 155 156 157 158 159 160 161	near M2 at 36°40'N and 122°25'W and 1800 m depth (Fig. 1). The mooring included an upward looking 300 kHz RD Instruments ADCP at 300 m depth, two current meters at 305 m and 1200 m depth and two sediment traps just below each current meter. Deployments lasted for five to six months except the last deployment which was for 10 months (Table 1). In the following sections, measurements at the upper (lower) level will be referred to as "300 m" ("1200 m") nominal depth. Aanderaa recording current meters (RCM8) were used. Current speed was measured by rotations of a shrouded paddle-type rotor which was magnetically linked to an electronic counter and current direction was measured by magnetic compass. Before deployment, the compass was calibrated and the counter tested for accuracy and proper operation in the				

164 minute intervals. Further details regarding current measurements are given by Aguilar-Morales165 (2003).

166 Two sequential sediment traps were used in this study (Table 1). One was an Indented 167 Rotating Sphere (IRS) sediment trap (Peterson et al., 1993) which was deployed at 320 m. The 168 second was a Honjo Mark VI sediment trap (Honjo and Doherty, 1988) at ~1205 m. Traps were 169 pre-programmed to sample the fluxes of sinking particles over approximately 14 days for all 170 deployments except the last, for which the sampling interval was 28 days. Gaps in the sediment 171 trap time-series were due to technical issues related to failure of the sediment trap program as 172 well as analytical issues described in the following section. All sediment traps were thoroughly 173 acid-cleaned before the deployment. In the laboratory, the rotary collector was cleaned with 174 detergent, soaked in HCl overnight, and rinsed several times with distilled water. Once at sea, 175 the traps were rinsed with seawater. The receiving cups were filled with seawater with a NaCl 176 excess of 5 g L⁻¹ and poisoned with 3.0 mM of mercury chloride to avoid degradation of 177 collected particles and disruption by swimmers (including organisms that did not fall 178 gravitationally through the water column; Thunell et al., 2000). Upon recovery, the receiving 179 cups were stored in the dark at 4°C until they were processed.

180

181 2.3. Sample processing and analytical techniques

182

183 In the laboratory, swimmers were removed from the samples by using fine tweezers under a 184 dissecting microscope. When necessary, the samples were divided into aliquots using a high-185 precision wet sample divider (Mc Lane-WSD-10). The WSD-10 divided a wet particle sample 186 into five or ten equal splits. To remove salts, the splits were rinsed with cold distilled water, 187 centrifuged and the supernatant eliminated. Samples were then dried in a 60°C oven for 24 h. 188 Dry splits were firstly used to calculate total mass fluxes. For total and organic carbon and 189 nitrogen elemental composition analysis, approximately 20 mg subsamples of dry split were 190 used. Subsamples for organic carbon were first decarbonated with repeated additions of 50 μ L 191 of HCl 15%. Total and organic carbon and nitrogen were measured with a Carlo-Erba NA-1100

192	analyzer. Sample analysis errors were generally 1% for carbon and nitrogen content. For a few
193	periods, sample material was not sufficient for analysis (Table 1). For IRS samples of
194	deployments nº 7 and 10, there were no samples due to analytical problems. Assuming all the
195	inorganic carbon was calcium carbonate (CaCO ₃), the CaCO ₃ content was estimated as [(total
196	carbon – organic carbon) \times 8.33].
197	
198	2.4. Offshore Ekman transport
199	
200	Offshore Ekman mass transport per meter of coastline, kg m ⁻¹ s ⁻¹ , was used as an index
201	of strength of upwelling (Schwing et al., 1996). The offshore transport estimate was based upon
202	6-hour charts of synoptic weather produced by the U.S. Navy Fleet Numerical and
203	Oceanography Center. The Ekman transports (and wind stress curl) were downloaded from
204	http://upwell.pfeg.noaa.gov/erddap/griddap/erdlasFnWPr.html for 36.5°N, 122.5°W (location
205	shown on Fig. 1) from 1998-2005. Missing values were replaced by linear interpolation, and
206	rotated so that offshore (negative) transport was directed perpendicular to the coast (toward
207	240°T).
208	
200	
210	3. Results
211	
212	3.1. Monterey Bay time series
212	5.1. Monterey Day and series
210	The time series of offshore Ekman transport, temperature, salinity, nitrate and primary
215	production in the upper 200 m for the period 1998 to 2005 are shown for station M2 in Fig. 2.
216	Time series of Ekman transport (Fig. 2A) clearly marked the upwelling season between
217	February and September. In addition, there was large interannual variability also seen in the

thermohaline and biogeochemical properties. The most negative (offshore) Ekman transport

occurred during the 1999 La Niña event and the maximum (onshore) during the 1998 El Niño
event (Fig. 2A). In fact, the most intense downwelling favouring winds were observed at the
beginning of 1998, during El Niño.

222 Despite the large interannual variability in water column temperature, mostly due to the 223 warm 1998 El Niño and the cold 1999 La Niña, there was also marked seasonality for the study 224 years (Fig. 2B). For each year, lowest temperatures at the sea surface were reached between 225 March – April (<12.0°C) and were warmest between July and September (>13.5°C). However, 226 year 2000 was characterized by relatively homogenous temperature ($12.5 \pm 1.1^{\circ}$ C) in the upper 227 50 meters of the water column for the entire year.

228 The salinity time series consisted of an annual cycle modulated by large interannual 229 variability (Fig. 2C). The 1998 El Niño and 1999 La Niña years were both characterized by 230 large salinity variability at the sea surface, ranging from a minimum of 32.2 in March of both 231 years and maximum of 33.5 (33.7) in May 1998 (July 1999), decreasing slightly, 0.1 (0.2), for October. However, from 2000 to 2002, sea surface salinity values were nearly homogeneous 232 233 and relatively salty for the entire year (33.51 ± 0.14) , except for the last four months of 2002. In 234 fact, there was a sharp decrease in salinity with a deepening of the halocline in September of 2002 through 2005, so that upper ocean salinities were lower (<33.2) than previous years. 235

The strong perturbation of the 1997 - 1998 El Niño was easily identified in the nitrate time series (Fig. 2D) by low nitrate levels ($<5 \mu$ M) and a deep nitracline for the entire year. For other years, high nitrate levels reaching the upper levels of the water column were registered during the upwelling season though with interannual differences. In 2002, nitrate levels higher than 10 μ M persisted for the entire upwelling season. In contrast, nitracline depth did not outcrop and reached only 20 m depth in May 2000.

Primary production values tracked thermohaline and chemical conditions (Fig. 2E). The
annual maximum values of primary production were observed during the upwelling season,
mainly during March - September, and minimum values during winter. There was also large
interannual variability and during the last three years relatively higher primary production

values were observed including the remarkably large value of integrated primary production of
228 mg m⁻² day⁻¹ (not shown) in the photic zone during August 2003.

248

- 249 *3.2. Monterey Bay vertical flux time series*
- 250

251 The complete time series of total mass, organic carbon (Corg) and CaCO₃ observed from 252 1998 through 2005 at 300 m and 1200 m depth are presented in Figs. 3 and 4. At 300 m depth, total mass flux varied from a minimum value of 22.1 mg m⁻² day⁻¹ to a maximum of 4502 mg m⁻ 253 254 2 day⁻¹ (Fig. 3A) The mean downward flux averaged over the entire study period was 762 ±660 mg m⁻² day⁻¹. Organic carbon fluxes ranged between a minimum of 4.1 mg m⁻² day⁻¹ and a 255 256 maximum value of 296 mg m⁻² day⁻¹ for September 1998, with an average flux for the entire 257 study period of 52 \pm 41 mg m⁻² day⁻¹ (Fig. 3B). In general, maximum peaks of C_{org} flux which 258 occurred at the same time as maximum values of primary production occurred during the EU 259 season from February to April (April 1998, May 1999, April 2001, April 2002, March 2003, 260 April 2004, March 2005). However, there were other maximum pulses of Corg flux not 261 associated with maximum values of primary production, as in December 1999, February 2001, February 2002 and October 2002. Fluxes of Corg followed a similar temporal trend to total mass 262 263 fluxes with a Pearson correlation coefficient of 0.77. Temporal variability of CaCO₃ flux was 264 similar to C_{org} flux, with an average of 75 ±62 mg m⁻² day⁻¹ for the entire study period (Fig. 3C). Although CaCO₃ fluxes corresponded to variations in C_{org} and total mass fluxes (r= 0.51 and 265 266 0.52 respectively), there were some peaks of Corg flux not reflected by CaCO3 pulses as in September 1998, February 2002, April 2004 and March 2005. Likewise, there were other peaks 267 268 in CaCO₃ fluxes that occurred simultaneously with lower fluxes of Corg such as observed in 269 December 1998 and May 2000.

At 1200 m depth, total mass flux varied from a minimum value of 0.2 mg m⁻² day⁻¹ to a maximum of 2580 mg m⁻² day⁻¹ (Fig. 4A). Organic carbon fluxes varied between a minimum of 0.1 mg m⁻² day⁻¹ and maximum of 142 mg m⁻² day⁻¹, with an average for the study period of 44 ± 28 mg m⁻² day⁻¹ (Fig 4B). These fluxes followed a similar temporal evolution of C_{org} fluxes at 274300 m, with a significant Pearson correlation coefficient of 0.47 between the two time series. In275fact, maximum pulses of C_{org} at 1200 m corresponded to maximum pulses at 300 m, as observed276in April 1998, September 1998, August 1999, April 2002, October 2002, April 2003 and April2772004. In contrast, maximum peaks of C_{org} at 300 m during the DV season from November to278January (December- 1999, February 2001 and February 2002) were not reflected in maximum279peaks at 1200 m. At 1200 m fluxes of CaCO3 (Fig. 4C) correlated with fluxes of total mass and280 C_{org} with Pearson correlation coefficients of 0.64 and 0.57, respectively.

Regarding the composition of settling material, the percentage of Corg relative to total 281 282 mass for the shallower trap varied between a minimum of 1.8% and maximum value of 18.6%, 283 with an average value of 7.8 \pm 3.2% for the entire study period (Fig. 3D). The percentage of C_{org} 284 in the deepest trap was significantly lower than for the shallower trap with an average value of 285 $5.3 \pm 1.5\%$ (Fig 4D). The highest percentages of C_{org} were registered during the OC season from 286 August to October at both trap levels. The Corg:N molar ratio ranged from 6.2 to 13.7 (average 287 8.6 ± 1.2) at the shallower level (Fig. 3D). At 1200 m, average C_{org}:N molar ratio (8.9 ± 1.0) was 288 not significantly different from the shallower trap (Fig. 4D).

289

290 *3.3. Annual cycles*

291

292 The mean annual cycle of wind-driven offshore Ekman transport for 1998 – 2005 is 293 shown in Figure 5A. The annual cycle accounts for 76% of the observed variance of the 294 offshore Ekman transport. The mean annual cycle of Ekman transport is directed offshore for all 295 but 19 days in late January when weak onshore transport occurs. Maximum (e.g. onshore) transport is 17 kg m⁻¹ s⁻¹ on January 20 and subsequently decreases monotonically to strongly 296 negative (e.g. offshore) transport of -1296 kg m⁻¹ s⁻¹ on June 3. It then takes seven and a half 297 298 months for the winds to increase to their January maximum. Assuming a Rossby radius of 20 299 km, the minimum transport corresponds to an upwelling rate of 8 m day⁻¹. The seasonal variability and the annual cycles of the thermohaline properties, nitrate and primary production 300 301 off Monterey Bay have been described in detail by Pennington and Chavez (2000), as

previously mentioned. Note the two maxima in primary production (Fig. 5B) during theupwelling period, centred on April 15 and August 5.

304 The annual cycle of currents and temperature at 300 m illustrates the physical response 305 to wind forcing at the location of the upper sediment trap (Fig. 5C - D). At the start of the year, 306 the mean currents are directed poleward, and subsequently slow to 1 cm s⁻¹ on March 19. The 307 poleward flow then increases to a maximum velocity, 9.3 cm s⁻¹, on June 13, ten days after the 308 offshore directed Ekman transport is greatest. The mean annual 300 m alongshore currents subsequently decrease to -0.5 cm s⁻¹ on October 10. Note that alongshore currents are directed 309 310 poleward for all but 28 days which are centred on this minimum. The annual cycle of 311 alongshore flow at 300 m accounts for 24% of the variability of the alongshore flow. Unlike 312 Ekman transport, the alongshore current velocity has secondary minima and maxima. The mean 313 annual cycle of temperature at 300 m (Fig. 5D) resembles the annual cycle of Ekman transport 314 at the start of the year: the temperature is 7.8°C on January 22 and subsequently decreases as the upwelling favourable transports increase. Minimum temperatures (7.1°C) occurs on May 6, 315 316 about a month before the offshore transport peaks, and subsequently reaches a maximum value 317 of 7.8°C on August 10, about 2 months after the poleward velocities are largest. The May cooling appears to be a response to upwelling, and the subsequent warming a response to the 318 319 increasing strength of the poleward flow of equatorial waters. For temperature, the mean annual 320 cycle accounts for 44.6% of the low frequency variability. The annual cycle of alongshore 321 currents at 1200 m at S2 (Fig. 5E) are southward all year round except for a few days centered 322 on May 5. Maximum southward speed is 3.1 cm s⁻¹ on July 18, a few days after the maximum 323 poleward current at 300 m. The annual cycle of temperature at 1200 m (Fig. 5F) only varied 324 0.11 °C for the entire year but this warming occurred between June 29 (minimum temperature 325 3.43°C) and June 29 (maximum temperature 3.54°C) about the same time the current 326 accelerated to maximum southward flow.

327 For the settling material at the two sediment trap levels, seasonal averages are calculated 328 for the four seasonal periods defined by Pennington and Chavez (2000) (Fig. 6). At 300 m, total 329 mass flux is significantly higher during EU (1129 \pm 929 mg m⁻² day⁻¹; p<0.05) compared with

330	the other three seasons; while the lowest total mass flux corresponds to DV season (Fig 6A).
331	Organic carbon fluxes follow a slightly different seasonal pattern with significantly higher
332	values during the EU and OC seasons (60 ±43 mg m ⁻² day ⁻¹ and 68 ±60 mg m ⁻² day ⁻¹
333	respectively) (Fig. 6B). Average seasonal fluxes of CaCO ₃ do not show any significant
334	differences amongst seasons (Fig. 6C). Due to the high total mass flux average for EU, the
335	percent C_{org} for this season is significantly lower (6 ±1%) than for other seasons (Fig. 6D), as
336	discussed further in section 4.3. Maximum average percent of C_{org} is 10 ±4% during the OC
337	season. The C_{org} : N and C_{org} : C_{inorg} ratio are not significantly different amongst the seasons and
338	range from 8.5 \pm 0.8 to 8.8 \pm 1.1 (Fig. 6D) and 5.7 \pm 3.5 to 7.2 \pm 3.3 (Fig. 6E), respectively.
339	At 1200 m, seasonal particle fluxes of total mass and C_{org} are not the same as at 300 m
340	(Fig. 6F-G). Maximum seasonal fluxes are found during the LU season from May to July (1194
341	\pm 568 mg m^{-2} day^{-1} and 59 ± 31 mg m^{-2} day^{-1} for total mass and C_{org} respectively) and, as at 300
342	m, minimum values occur during the DV season (526 ±495 mg m $^{-2}$ day $^{-1}$ and 28 ±20 mg m $^{-2}$
343	day-1 for total mass and organic carbon respectively). Likewise, maximum seasonal flux of
344	$CaCO_3$ (101 ±50 mg m ⁻² day ⁻¹) occurs during the LU season but is only significantly different
345	from the DV seasonal flux (Fig. 6H). Regarding the quality of settling material, as at 300 m, the
346	highest C_{org} content is for the OC season (6 ±1%); while C_{org} :N ratio is not significantly
347	different for the four seasons (Fig. 6I). The seasonal average C_{org} : C_{inorg} ratio varies between 4.1
348	± 2.4 for EU and 6.2 ± 4.1 for OC, being significantly different between these two seasons
349	(p<0.05) (Fig. 6J).
350	
351	
352	4. Discussion
353	
354	This study examines the biological pump offshore of Monterey Bay through 2 time series
355	of vertical carbon flux as captured by sediment traps. A discussion of the efficiency of the
356	deployed sediment traps is first presented. Subsequently, the discussion focuses on the vertical
357	flux of C_{org} and its temporal (seasonal and interannual) and vertical (300 and 1200 m) variability

to evaluate the fate of particulate organic carbon. Finally, a seasonal one dimensional (1D)

359 budget of organic carbon in this coastal upwelling system is presented.

360

361 *4.1. Quality of trap fluxes*

362

The use of sediment traps has contributed significantly to the study of vertical particulate matter flux in the oceans. However, trap collection efficiency has been questioned because of potential hydrodynamic bias due to current speed (Gardner et al., 1997; Buesseler et al., 2007), and associated errors due to trap tilting (Gardner, 1985). To address these issues, a brief quality assessment of the trap fluxes reported here is given below.

368 Gardner (1980) indicated that cylindrical traps, such as the IRS and Honjo Mark VI used

369 here, experience a negligible reduction of collection efficiency of vertical fluxes in flows up to

370 15 cm s⁻¹. Subsequently, Gardner et al. (1997) found that in the field, cylindrical collectors with

high aspect ratios (>2) should produce little bias in current speeds as large as 22 cm s^{-1} .

372 Average current speeds at 300 m for each season are shown in Table 2 with mean current speeds

of 3.7 - 18.6 cm s⁻¹. Mean current velocities above 15 cm s⁻¹ (Gardner, 1980; Antia et al., 1999;

Heussner et al., 2006) were observed during the LU season of all years and during two OC

seasons. During LU, the percentage of time with currents above 15 cm s⁻¹ ranged between 20%

in year 2002 to 60% during the La Niña year of 1999, when strong northerly winds were

377 persistent. During the OC, only 2000 and 2002 experienced speeds above 15 cm s⁻¹. At 1200 m

depth, average current speeds were much lower than 15 cm s⁻¹, ranging between 1.2 - 5.3 cm s⁻¹

379 (Table 2). Following Gardner et al. (1997), if strong hydrodynamic biases due to current

380 intensity had occurred, either high fluxes should be expected when currents were strong

381 (overcollection) or, conversely, low fluxes when currents were weak (undercollection).

382 However, correlation coefficients of total mass flux vs current speed for each of the four seasons

383 were not statistically significant (r > 0.2); this indicated that particulate matter fluxes were not

384 significantly biased by horizontal current speeds.

Trap inclination to the vertical can also affect trap efficiency (Gardner, 1985) but inclination was limited by mooring design. Figure 7 shows the relationship between mooring tilt and current speed at 300 m for 15 minute samples. The tilt angle was less than 0.8° at velocities ~ 40 cm s⁻¹, indicating that the sediment trap was very stable and that inclination probably did not affect efficiency

Thus, even though high current speeds during the late upwelling season could have influenced the efficiency of the 300-m sediment trap, the very low inclination of the mooring line and the absence of correlation between mean current speed and mass of sinking material suggested that the sediment trap data were not biased by hydrodynamic effects.

394

395 *4.2. Seasonal and interannual variability of the vertical fluxes*

396

This 7.3-year study of particle flux off Monterey Bay spanned very different oceanographic
conditions including (1) the last phase of the strong 1997 – 1998 El Niño, (2) the subsequent
cold 1999 – 2000 La Niña, and (3) the anomalous onshore presence of Subarctic waters between
2002 and 2005. Although there were gaps in the sediment trap observations, the data provide
insights about the vertical export organic carbon from the photic zone.

In general, C_{org} flux measured at station M2 40 km offshore of Monterey Bay (52 and 44 mg m⁻² day⁻¹ at 300 m and 1200 m respectively) were similar to those previously reported by Pilskaln et al. (1996) at station S1 at the mouth of Monterey Bay (40 mg m⁻² day⁻¹; Fig. 1). For other coastal margins, Thunell et al. (2007) reported an average C_{org} flux in Santa Barbara Basin (~315 km south of Monterey Bay) of 96 mg m⁻² day⁻¹, nearly twice that of Cariaco Basin and 4 times higher than Guaymas Basin, with all three sites having C_{org} flux significantly higher than the open ocean average (7 mg m⁻² day⁻¹ for the depth interval from 250 to 500 m).

409 Vertical fluxes of C_{org} off Monterey Bay were lowest during the DV season, though not

410 significantly different from the LU season, and maxima for the EU and OC seasons at 300 m

411 depth. This seasonal variation seemed to reflect biological control, and should be related to the

412 seasonal cycle of primary production in the region in response to coastal upwelling. In addition,

413 the relatively low Corg: N ratio for all seasons (ranged between 8.5 and 8.8) suggested a marine 414 origin of the sinking particulate matter, in contrast to the C:N ratio greater than 20 found for 415 organic matter from terrestrial sources (Emerson and Hedges, 1988). However, the direct 416 comparison of Corg flux and primary production for the studied years did not result in a close relationship (r = 0.12), mainly due to the LU data with high primary production and low C_{org} 417 fluxes (Fig. 8). This apparent decoupling between Corg flux and primary production suggests that 418 419 other factors must influence Corg fluxes at depth. In fact, it is well established that strong 420 upwelling-favorable, southward winds promote the formation of upwelling filaments in which 421 large fractions of the biogenic particles from the continental shelf are transported offshore 422 (Suess, 1980; Walsh, 1991; Thunell, 1998; Olli et al., 2001). Chavez et al. (2002) indicates that 423 the productive area is extended offshore during the summer due to offshore flow in upwelling 424 filaments. The seasonal variability in the vertical fluxes of Corg off Monterey Bay may be related 425 to this transport, as follows (Fig. 9). Under strong offshore Ekman transport, rates of horizontal offshore export of the fixed organic carbon was high, often producing low vertical Corg fluxes, 426 427 even in those situations with relatively high primary production. Stated simply, when Ekman 428 transport is high, vertical export tends to be low (Fig. 9). In contrast, under weak offshore 429 Ekman flow, horizontal export is low and vertical transport becomes more important, and more 430 events with high C_{org} vertical fluxes were observed.

431 Zooplankton may also affect vertical fluxes of Corg by reprocessing material into fecal 432 pellets. In his review of biological pump studies, Turner (2015) indicated that fecal pellets are 433 often recycled in the upper few hundred meters of the water column by coprophagy and 434 bacterial decomposition. Off Monterey Bay, maximum zooplankton abundance occurs during 435 summer (Marinovic et al., 2002; Croll et al., 2005; Chavez et al., this issue). Consequently, 436 maximum zooplankton feeding rates should be expected during the LU season, perhaps 437 decoupling LU primary production peaks and reducing sinking C_{org} during this season. 438 In addition to seasonality, the study also spans very different interannual conditions, 439 modulated by both local and large scale forcing (Chavez et al., 2011; Pennington and Chavez, 440 this issue). As previously pointed out, the region was strongly influenced by the strong 1997-

441 1998 El Niño followed by an intense 1999-2000 La Niña period. After 2001, there was a 442 strengthening of the California Current, reflected here by low salinity waters at station M2 (Fig. 443 2C), associated with an intensification of the North Pacific Gyre oscillation. Di Lorenzo et al. 444 (2008) have shown that a positive North Pacific Gyre Oscillation indicates a strong Alaska 445 Subpolar and North Pacific Subtropical Gyre, and strong California Current and coastal 446 upwelling. This variability clearly affected the primary production of the Central California 447 coastal upwelling system (Chavez et al., 2011), and to some extent, must be manifested in the interannual variability of Corg fluxes. Unfortunately, it was not possible to determine annual 448 449 averages of Corg fluxes for the study years due to data gaps. Sampling coverage was less than 450 50% of the annual cycle for some study years, but it was possible to determine averages for the LU seasons for all the different years (Fig. 10). When Corg fluxes for the LU seasons of each 451 year were compared, the lowest Corg fluxes occurred during years 1999, 2000 and 2001, in 452 453 association with La Niña. In contrast, the Corg flux for the LU season of the 1998 El Niño year 454 was similar to the Corg flux observed during 2002 through 2004. The LU seasons of 2003 and 455 2004 were characterized by an unusual onshore intrusion of the California Current, as also 456 described for LU season of 1998 (Chavez et al., 2002; Collins et al., 2002). This anomalous 457 shift of the California Current prevented the offshore horizontal transport of particulate organic 458 matter present over the shelf, likely enhancing vertical export. In contrast, during La Niña years 459 (1999, 2000 and 2001) intense upwelling-favorable winds enhanced horizontal export of particulate organic matter, likely reducing vertical Corg fluxes. 460

461

462 4.3. Attenuation of vertical organic carbon fluxes

463

Rapid biological consumption and remineralization of carbon in the mesopelagic zone
(depths between the euphotic zone and 1000 m) reduce the flux carbon to depth (Buesseler et
al., 2007). The comparison of vertical particle flux between the 300 m and 1200 m sediment
traps provides an assessment of this vertical attenuation of sinking material. In this way, the
'efficiency' of the Central California coastal upwelling system in the transfer of organic carbon

469 from the upper layers into the deep sea can be determined and thus the ability of this ecosystem470 to take up atmospheric CO₂ assessed.

471 Vertical attenuation of Corg fluxes was observed for all seasons except the LU. This vertical 472 attenuation varied from 31% during the OC season to 24% for the DV season. These 473 percentages are not high, revealing a system that efficiently moves organic carbon from the 474 upper layers with relatively little remineralization of organic carbon in the mesopelagic zone. 475 Attenuation ranges were similar to those previously described by Buesseler et al. (2007) at the 476 mesotrophic site of the Western Subarctic Gyre (43% - 53%) but are much lower than 477 attenuation found at an oligotrophic site in the North Pacific Subtropical Gyre (~80%). The 478 lower attenuation in the Subpolar Gyre was attributed to fast sinking of dense fecal pellets 479 containing high proportions of ballasting biominerals, mainly biogenic silica. 480 The flux attenuation off Monterey Bay thus resembles that in the Subarctic Gyre and we 481 hypothesize that similar controlling factors regulate flux. Off Monterey Bay, the phytoplankton 482 community in the photic layer was mainly dominated by diatoms, which were the main 483 contributors to the high primary production of the region (Pennington et al., 2010; Chavez et al., 484 this issue). Unfortunately, no biogenic silica data are available for the present sediment trap time 485 series, but Monterey Bay measurements by Pilskaln et al. (1996) found high opal content. Silica 486 was the largest contributor to biogenic material (average content of 17%) and had the highest 487 correlation with C_{org} fluxes, supporting the idea that biogenic silica was the main ballast 488 biomineral in this coastal upwelling system. In addition, Pilskaln et al. (1996) described an 489 abundance of centric diatom valves within zooplankton fecal pellets in the sediment trap 490 material during the upwelling months, suggesting a vertical C_{org} export mechanism similar to 491 that described for the Western Subarctic Gyre (Honda et al., 2006; Buesseler et al., 2007). 492 Oxygen may also affect flux attenuation. Several authors (Devol and Hartnett, 2001; Van 493 Mooy et al., 2002) suggested that low oxygen conditions greatly increase the amount of carbon 494 transferred to the deep ocean due to decreased oxidation rate of the sinking material. Devol and Hartnett (2001) determined an attenuation of only 38% for the Mexican margin in comparison 495 to 70% through a more typical oxic water column off Washington. Off Monterey Bay, a strong 496

497 oxygen minimum with oxygen levels $< 20 \ \mu$ mol kg⁻¹ occurs between 500 m and 1000 m (Castro 498 et al., 2001); conditions which could inhibit oxidation of sinking C_{org}. However, the water 499 column between the two sediment traps also included well-ventilated upper waters, where 500 heterotrophic activity and, consequently, oxidation of organic carbon takes place. Thus, the 501 extent to which the presence of suboxic waters may have inhibited degradation of sinking 502 organic matter cannot be ascertained. Additional studies are necessary to unravel the role of low 503 oxygen concentrations on the carbon transfer off Central California.

504 During the LU season, 41% higher Corg fluxes were observed at 1200 m than at 300 m. This 505 large flux at the deepest trap remains enigmatic, but could have been due to lower efficiency of 506 the shallower trap during this season (see section 4.1) or to the collection of resuspended 507 material. Sediments deposited on continental margins are prone to resuspension by vigorous 508 bottom currents (Rea and Hovan, 1995). The strongest currents at both 300 and 1200 m off 509 Monterey Bay occur during the LU season, being northward at 300 m and southward and 510 offshore at 1200 m (Fig. 5C-E), producing the largest vertical shear. These dynamics could have 511 resulted in resuspension and lateral offshore transport of slope sediment. Canyon sediment 512 transport processes, such as slumping, turbidity flows and gravity flows are very active in the Monterey Canyon (Eittreim et al., 2002; Farnsworth and Milliman, 2003) and move sediment 513 514 discharged from Salinas River oceanward (Paull et al., 2002, Xu et al., 2002). Alternatively, 515 resuspended material could have been advected southwards from the Gulf of Farallones or by 516 resuspension episodes similar to those documented at station M about 65 km southwest of 517 Monterey Bay (Baldwin et al., 1998; Hwang et al., 2004). Hwang et al. (2010), based upon a compilation of C_{org} and ¹⁴C of sinking material, estimated that 35% of C_{org} may derive from 518 519 resuspended sediments globally, suggesting an important role of the resuspension of 520 sedimentary organic matter and subsequent lateral transport in the export of organic carbon to 521 the deep ocean. Further studies based on carbon isotope ratios are necessary to clarify the origin 522 and impact of this resuspended material off Monterey Bay, considering also the potential 523 contribution from sediment discharge from either the Salinas or Sacramento Rivers.

524 The ratio of particulate organic carbon to particulate inorganic carbon (Corg: Cinorg) of the 525 exported material can also influence the carbon – sequestering efficiency of the biological pump 526 (Tsunogai and Noriki, 1991; Wong et al., 1999; Antia et al., 2001; Honda et al., 2002), since 527 carbon fixation by photosynthesis decreases and calcification have opposite effects on water 528 column CO₂ (Tsunogai and Noriki, 1991; Frankignoulle et al., 1994). In contrast to 529 photosynthesis, the formation of one mole of CaCO₃ releases approximately 0.6 moles of CO₂. 530 Thus, the partial pressure of CO_2 is drawn down when photosynthesis exceeds $CaCO_3$ formation in surface waters (e.g. when Corg: Cinorg >0.6 (Tsunogai and Noriki, 1991; Frankignoulle et al., 531 1994). In this way, high Corg: Cinorg ratios indicate preferential carbon fixation as Corg rather than 532 Cinorg favoring the biological pump as a mechanism for drawing atmospheric CO2 into the ocean 533 (Wong et al., 1999). For our sediment traps, the Corg: Cinorg ratio was relatively high, averaging 534 535 6.5 and 5.1 for 300 m and 1200 m, respectively, indicating that the study site acted as a sink of 536 CO₂ on annual basis

537 Overall, the sediment trap data reveal an efficient transfer of organic carbon towards the 538 sediment as supported by the relatively low attenuation of vertical fluxes for all seasons except 539 late upwelling and the relatively high C_{org} : C_{inorg} ratio of sinking material at both 300 and 1200 540 m.

541

542 4.4. Seasonal POC budget for Monterey Bay

543

544 To summarize these results, a seasonal one dimensional (1D) vertical budget of Corg for 545 Monterey Bay was produced (Fig. 11), using the measured primary production and vertical 546 fluxes at 300 and 1200 m. In this way, the annual budget previously established by Pilskaln et al. (1996) was divided into seasons. Unfortunately, the photic zone export flux, i.e. the amount 547 548 of Corg vertically exported from ~100 m, was not measured in spite of being a critical 549 component of the Corg budget. Thus, these vertical fluxes have been estimated using published 550 primary production and export flux observations in the California coastal upwelling region 551 (Small et al., 1989; Pilskaln et al., 1996; Stukel et al., 2015). Calculated e-ratios, from these

552 contemporary measurements of primary production and export flux, decrease with increasing primary production, as previously indicated by several authors (Pilskaln et al., 1996; Pennington 553 554 et al., 2010; Stukel et al., 2013). Based on the best fit of e-ratio with primary production (PP) using the available data (e-ratio = $6.425 \text{ x PP}^{-0.507} \text{ r}=0.47$), the C_{org} flux at 100 m for each season 555 556 was estimated. These 100 m fluxes accounted for between 25% and 18% of primary production, 557 with maximum e-ratio values during the less productive DV season and a mean annual e-ratio of 558 0.19. Pilskaln et al. (1996) obtained the same e-ratio based on primary production and sediment 559 trap data collected in Monterey Bay from 1989 through 1992 (see their Fig. 10). 560 In these seasonal 1D budgets, part of the export fluxes continues settling through the water column in such a way that the amount of Corg captured at the 300-m sediment trap constituted 561 562 between 20% for the LU season and 32% for the EU and OC seasons of the estimated 100 m 563 export fluxes, slightly higher than the annual mean of 18% obtained by Pilskaln et al. (1996). In 564 terms of primary production, Corg flux at 300 m represented between 6.4% and 3.5% for the EU 565 and LU seasons respectively. The lower percentage for the LU season must be due to either (1) 566 increased horizontal export of material offshore in upwelling filaments or (2) intense 567 heterotrophic processes between 100 m and 300 m (section 4.2). Several authors have described 568 maximum attenuation of vertical fluxes corresponding to this layer just above the oxycline 569 (Martin et al., 1987; Antia et al., 2001; Henson et al., 2011). If the difference in Corg flux 570 between 100 and 300 m was wholly due to heterotrophic processes, remineralization rates in 571 this depth range varied from 117 mg m⁻² d⁻¹ during the DV season to 171 mg m⁻² d⁻¹ for LU season, not too different from the annual average of 177 mg m⁻² d⁻¹ estimated by Pilskaln et al. 572 (1996). 573 574 The organic carbon remineralization rates can be estimated from the difference between C_{org}

fluxes for the two sediment trap depths. Excluding the LU season, when C_{org} flux at 1200 m was higher than C_{org} flux at 300 m, as previously discussed (section 4.3), C_{org} remineralization rates varied between 9 mg m⁻² d⁻¹ during the DV season and 21 mg m⁻² d⁻¹ for the OC season. These values are somewhat lower than the average C_{org} remineralization rate (35.2 – 24.3 mg m⁻² d⁻¹) estimated by Sonnerup et al. (2013) for the main thermocline of the NE Pacific based on oxygen tilization rates determined on isopycnals from 26.0 to 27.0 kg m⁻³ σ_{θ} and considering a

respiration coefficient ranging from 1 to 0.7, respectively. In the present data, there seems to be

- 582 a seasonal variability of deep-water remineralization affected by temperature. At higher average
- 583 temperature during the OC season, C_{org} remineralization was higher and at a minimum during
- the DV season.

585 The Corg flux at 1200 m can be considered as the 'rain flux', i.e. the amount of Corg arriving 586 at the surface sediment. Seasonal averages ranged between 28 mg m⁻² d⁻¹ for DV and 59 mg m⁻² 587 d⁻¹ for LU. These values are higher than the average annual seafloor carbon flux of 19.7 mg m⁻² 588 day-1 reported by Pilskaln et al. (1996) based on benthic chamber and microelectrode 589 measurements of oxygen, TCO₂ and carbonate alkalinity. However, our values were similar to the Corg rain to the seafloor of 34.8 and 45.6 mg m⁻² d⁻¹ derived by adding the oxidation rates 590 and Corg burial rates used by Berelson and Stott (2003). The Corg fluxes at 1200 m also included 591 592 seasonal variability with minimum values during the winter months reflecting minimum values 593 of primary production during this season. For the four seasons, Corg flux at 1200 m represented 594 about 4.0%- 4.9% of the primary production.

595

596

597 5. Conclusions

598

599 This study describes the flux of photosynthetically fixed organic carbon to the deep sea 600 off Monterey Bay. On a seasonal scale, the vertical flux of Corg at 300 m represents around 3.5% - 6.4% of the fixed carbon. Low values of flux of Corg occur during the LU season from May to 601 602 July, probably due to strong offshore Ekman transport and intense metabolic activity. The 603 sediment trap data at 300 m and 1200 m allowed evaluation of the attenuation of Corg flux 604 through the water column. Compared to other ecosystems, the attenuation of the vertical flux 605 signal was relatively low for all seasons (24 - 31%), except during the LU season, pointing to a 606 relatively unmodified and 'efficient' transfer of Corg through the mesopelagic layer by the

607 biological pump. Excess C_{org} was collected in the 1200 m sediment trap during the LU season for unknown reasons. It is possible that strong deep currents may resuspend continental shelf or 608 609 slope sediment, which is then advected offshore and captured by the trap. Unfortunately, it was 610 not possible to estimate the percent contribution of the resuspended material even though such 611 resuspension must be an important conduit of material to the deep ocean. The ratio of C_{org} flux 612 at 1200 m to surface primary production was estimated to be 4.0% to 4.9%. These transfer 613 efficiencies are in the upper range of previously reported values. In addition, the sinking material at 1200 m also presented relatively high Corg:Cinorg ratios. Thus, the analysis of the 614 615 temporal time series of sinking particulate matter provided evidence that a strong biological 616 pump in this coastal upwelling region efficiently sequesters atmospheric CO_2 in the deep sea.

In a changing ocean, coastal upwelling systems are critical regions as they constitute the most biologically productive marine ecosystems. An increasing trend in water column stratification and a decrease in the intensity and frequency of coastal upwelling, as reported by recent investigations, could result in less upwelling of nutrient-rich upwelled water and a potential shift of the microbial community structure towards the dominance of the nano- and picoplankton. These potential changes in the ecosystem functioning could completely modify the fluxes of C_{org} to the deep ocean.

624

625

626 ACKNOWLEDGMENTS

627

The principal source of support for these measurements was the David and Lucile
Packard Foundation. CGC was partially supported by a National Research Council Fellowship
at the Naval Postgraduate School. We would also like to acknowledge the efforts of the crew of
the *R/V Point Sur* in setting and retrieving the sediment trap moorings. We would also thank to

- 632 Marla Stone and Erich Rienecker for their capable assistance with sediment trap moorings, and
- 633 Reiko Michisaki for help with computing.

636 **References**

- Aguilar-Morales, J., 2003. Subtidal Circulation Over the Upper Slope to the West of Monterey
 Bay, California. Thesis. Naval Postgraduate School. Monterey, CA, 128 pp.
- Antia, A.N., Koeve, W., Fischer, G., Blanz, T., Schulz-Bull, D., Scholten, J., Neuer, S.,
 Kremling, K., Kuss, J., Peinert, R., Hebbeln, D., Bathmann, U., Conte, M., Fehner, U.,
 Zeitzschel, B., 2001. Basin-wide particulate carbon flux in the Atlantic Ocean: Regional
 export patterns and potential for atmospheric CO2 sequestration. Global Biogeochem. Cy.
 15(4), 845-862.
- Antia, A.N., von Bodungen, B., Peinert, R., 1999. Particle flux across the mid-European
 continental margin. Deep Sea Res., Part I. 46(12), 1999-2024.
- Asanuma, H., Rago, T. A., Collins, C.A., Chavez, F.P., Castro,C.G., 1999. Changes in the
 Hydrography of Central California Waters associated with the 1997–1998 El Niño.
 Technical Report NPS-OC-99-001, Naval Postgraduate School. Monterey, CA, 121pp.
- Baldwin, R. J., Glatts, R.C., Smith Jr. K.L., 1998. Particulate matter fluxes into the benthic
 boundary layer at a long time-series station in the abyssal NE Pacific: composition and
 fluxes. Deep Sea Res., Part II. 45(4-5), 643-665.
- Bauer, J., Cai, W.-J., Raymond, P.A., Bianchi, T.S., Hopkinson Jr, C.S., Regnier, P.A., 2013.
 The changing carbon cycle of the coastal ocean. Nature. 504, 61-70.
- Berelson, W. M., Stott, L.D., 2003. Productivity and organic carbon rain to the California
 margin seafloor: Modern and paleoceanographic perspectives. Paleoceanography. 18 (1),
 2-1-2-15.
- Buesseler, K. O., Antia, A.N., Chen, M., Fowler, S.W., Gardner, W.D., Gustafsson, O., Harada,
 H., Michaels, A.F., van der Loeff, M.R., Sarin, M., Steinberg, D.K., Trull, T., 2007. An
 assessment of the use of sediment traps for estimating upper ocean particle fluxes. J. Mar.
 Res. 65(3), 345-416.
- 661 Carr, M.E., 2003. Simulation of carbon pathways in the planktonic ecosystem off Peru during
 662 the 1997-1998 El Niño and La Niña. J. Geophys. Res.. 108(C12), 3380.
- 663 Castro, C.G., Chavez, F.P., Collins, C.A., 2001. Role of the California undercurrent in the
 664 export of denitrified waters from the eastern tropical North Pacific. Global Biogeochem.
 665 Cy. 15(4), 819-830.
- 666 Chavez, F., Messié, M., Pennington, J.T., 2011. Marine primary production in relation to
 667 climate variability and change. Ann. Rev. Mar. Sci. 3, 227-260.
- 668 Chavez, F.P., Pennington, J.T., Castro, C.G., Ryan, J.P., Michisaki, R.P., Schlining, B., Walz,
 669 P., Buck, K.R., McFadyen, A., Collins, C.A., 2002. Biological and chemical
 670 consequences of the 1997-1998 El Niño in central California waters. Prog. Oceanogr.
 671 54(1-4), 205-232.
- 672 Chavez, F.P., Sevadjian, J., Wahl, C., Friederich, J., Friederich, G., this issue Measurements of
 673 pCO2 and pH from an autonomous surface vehicle in a coastal upwelling system. Deep
 674 Sea Res., Part II.
- 675 Chen, C.T.A., Borges, A.V., 2009. Reconciling opposing views on carbon cycling in the coastal
 676 ocean: Continental shelves as sinks and near-shore ecosystems as sources of atmospheric
 677 CO2. Deep Sea Res., Part II. 56(8-10), 578-590.
- 678 Collins, C.A., Castro, C.G., Asanuma, H., Rago, T.A., Han, S._K., Durazo, R. Chavez, F.P.,
 679 2002. Changes in the hydrography of Central California waters associated with the 1997680 98 El Niño. Prog. Oceanogr. 54 (1-4), 205-232.
- 681 Collins, C.A., Pennington, J.T., Castro, C.G., Rago, T.A., Chavez, F.P., 2003. The California
 682 Current system off Monterey, California: physical and biological coupling. Deep Sea
 683 Res., Part II. 50(14-16), 2389-2404.
- 684 Croll, D.A., Marinovic, B., Benson, S., Chavez, F.P., Black, N., Termullo, R., Tershy, R., 2005.
 685 From wind to whales: trophic links in a coastal upwelling system. Mar. Ecol. Prog. Ser.
 686 289, 117-130.
- 687 Devol, A.H., Hartnett, H.E., 2001. Role of the oxygen-deficient zone in transfer of organic
 688 carbon to the deep ocean. Limnol. Oceanogr. 46(7), 1684-1690.

- bi Lorenzo, E., Schneider, N., Cobb, K.M., Franks, P.J.S., Chhak, K., Miller, A.J., McWilliams,
 J.C., Bograd, S.J., Arango, H., Curchitser, E., Powell, T.M., Riviêre, P., 2008. North
 Pacific Gyre Oscillation links ocean climate and ecosystem change. Geophys. Res. Lett.
 35(8).
- 693 Ducklow, H.W., Steinberg, D.K., Buesseler, K.O., 2001. Upper ocean carbon export and the
 694 biological pump. Oceanography. 14(4), 50-58.
- Emerson, S., Hedges, J.I., 1988. Processes controlling the organic carbon content of open ocean
 sediments. Paleoceanography. 3(5), 621-634.
- Falkowski, P.G., Flagg, C.N., Rowe, G.T., Smith, S.L., Whitledge, T.E., Wirick, C.D., 1988.
 The fate of a spring phytoplankton bloom: export or oxidation? Cont. Shelf Res. 8(5-7),
 457-484.
- Frankignoulle, M., Canon, C., Gattuso, J.-P., 1994. Marine calcification as a source of carbon dioxide: positive feedback of increasing atmospheric CO2. Limnol. Oceanogr. 39(2), 458-462.
- Gardner, W.D., 1980. Field calibration of sediment taps. J. Mar. Res. 38, 41-52.
- Gardner, W.D., 1985. The effect of tilt on sediment trap efficiency. Deep Sea Res., Part A.
 32(3), 349-361.
- Gardner, W.D., Biscaye, P.E., Richardson, M.J., 1997. A sediment trap experiment in the Vema
 Channel to evaluate the effect of horizontal particle fluxes on measured vertical fluxes. J.
 Mar. Res. 55(5), 995-1028.
- Gruber, N., Sarmiento, J.L., 2002. Large scale biochemical/ physical interactions in elemental
 cycles, in: Robinson, A.R., McCarthy, J.J., Rothschild, B.J (Eds.), The sea: Biologicalphysical interactions in the oceans. New York NY, John Wiley & Sons, pp. 337–399.
- Hansell, D.A., 2002. DOC in the global ocean carbon cycle, in: Hansell, D.A., Carlson, C.A.
 (Eds.), Biogeochemistry of marine dissolved organic matter. San Diego, Academic Press,
 pp. 685–715.
- Henson, S.A., Sanders, R., Madsen, E., Morris, P.J., Le Moigne, F., Quartly, G.D., 2011. A
 reduced estimate of the strength of the ocean's biological carbon pump. Geophys. Res.
 Lett. 38(4), doi: 10.1029/2011GL046735.
- Heussner, S., Durrieu de Madron, X., Calafat, A., Canals, M., Carbonne, J., Delsaut, N.,
 Saragoni, G., 2006. Spatial and temporal variability of downward particle fluxes on a continental slope: Lessons from an 8-yr experiment in the Gulf of Lions (NW
 Mediterranean). Mar. Geol. 234(1-4), 63-92.
- Honda, M.C., Imai, K., Nojiri, Y., Hoshi, F., Sugawara, T., Kusakabe, M., 2002. The biological
 pump in the northwestern North Pacific Ocean based on fluxes and major components of
 particulate matter obtained by sediment-trap experiments (1997-2000). Deep Sea Res.,
 Part II. 49(24-25), 5595-5625.
- Honda, M.C., Kawakami, H., Sasaoka, K., Watanabe, S., Dickey, T., 2006. Quick transport of
 primary produced organic carbon to the ocean interior. Geophys. Res. Lett. 33(16).
- Honjo, S., Doherty, K.W., 1988. Large aperture time-series sediment traps; design objectives, construction and application. Deep Sea Res., Part A. 35(1), 133-149.
- Hopkinson Jr, C.S., Vallino, J.J., 2005. Efficient export of carbon to the deep ocean through
 dissolved organic matter. Nature. 433(13), 142-145.
- Hwang, J., Druffel, E.R.M., Eglinton, T.I., 2010. Widespread influence of resuspended
 sediments on oceanic particulate organic carbon: Insights from radiocarbon and
 aluminum contents in sinking particles. Global Biogeochem. Cy. 24(GB4016).
- Hwang, J., Druffel, E.R.M., Griffin, S., Smith Jr., K.L., Baldwin, R.J., Bauer, J.E., 2004.
 Temporal variability of □¹⁴C, □¹³C, and C/N in sinking particulate organic matter at a deep time series station in the northeast Pacific Ocean. Global Biogeochem. Cy. 18(4), 9
 pp.
- 739 Inthorn, M., Wagner, T., Scheeder, G., 2006. Lateral transport controls distribution, quality, and
 740 burial of organic matter along continental slopes in high-productivity areas. Geology.
 741 34(3), 205-208.
- 742 IPCC, 2013. Climate Change 2013: The Physical Science Basis. Working Group I Contribution
 743 to the Fifth Assessment Report of the Intergovernmental Panel on Climate Change.

- 744 Stocker, T.F., Qin, D., Plattner, G.-K., Tignor, M.M.B., Allen, S.K., Boschung, J.,
- Nauels, A., Xia, Y., Bex, V., Midgley, P.M. (Eds.), Cambridge, Cambridge University
 Press. 1535 pp.
- Lampitt, R.S., Achterberg, E.P., Anderson, T.R., Hughes, J.A., Iglesias-Rodríguez, M.D., KellyGerreyn, B.A., Lucas, M., Popova, E.E., Sanders, R., Shepherd, J.G., Smythe-Wright, D.,
 Yool, A., 2008. Ocean fertilization: a potential means of geoengineering? Phil. Trans. R.
 Soc. A. 366, 3919–3945.
- Liu, K.-K., Atkinson, L., Quiñones, R., Talaue-McManus, L., (Eds.), 2010. Carbon and Nutrient
 Fluxes in Continental Margins. Global Change. Berlin Heidelberg, Springer- Verlag.
- Marinovic, B.B., Croll, D.A., Gong, N., Benson, S.R., Chavez, F.P., 2002. Effects of the 19971999 El Niño and La Niña events on zooplankton abundance and euphausiid community
 composition within the Monterey Bay coastal upwelling system. Prog. Oceanogr. 54(1-4),
 265-277.
- Martin, J.H., Knauer, G.A., Karl, D.M., Broenkow, W.W., 1987. VERTEX: carbon cycling in
 the northeast Pacific. Deep Sea Res., Part A. 34(2), 267-285.
- Muller-Karger, F.E., Varela, R., Thunell, R., Luerssen, R., Hu, C., Walsh, J.J., 2005. The
 importance of continental margins in the global carbon cycle. Geophys. Res. Lett. 32(1),
 1-4.
- Olli, K., Riser, C.W., Wassmann, P., Ratkova, T., Arashkevich, E., Pasternak, A., 2001. Vertical
 flux of biogenic matter during a Lagrangian study off the NW Spanish continental
 margin. Prog. Oceanogr. 51(2-4), 443-466.
- Passow, U., Carlson, C.A., 2012. The biological pump in a high CO2 world. Mar. Ecol. Prog.
 Ser. 470, 249–271.
- Pennington, J.T., Castro, C.G., Collins, C.A, Evans, W.W.I., Friederich, G.E., Michisaki, R.P.,
 Chavez, F.P., 2010. A carbon budget for the northern and central California coastal
 upwelling system, in: Liu, K.-K., Atkinson, L., Quiñones, R., Talaue-NcManus, L. (Eds.),
 Carbon and nutrient fluxes in Continental Margins. Global Change. Berlin Heidelberg,
 Springer-Verlag, pp. 29 -44.
- Pennington, J.T., Chavez, F.P., 2000. Seasonal fluctuations of temperature, salinity, nitrate,
 chlorophyll and primary production at station H3/M1 over 1989-1996 in Monterey Bay,
 California. Deep Sea Res., Part II. 47, 947-973.
- Pennington, T.P., Chavez, F.P., this issue- Interannual and Decade-Scale Oceanographic
 Fluctuation in Monterey Bay, California over 1989-2011. Deep Sea Res., Part II.
- Peterson, M.L., Hernes, P.J., Thoreson, D.S., Hedges, J.I., Lee, C., Wakeham, S.G., 1993. Field
 evaluation of a valved sediment trap. Limnol. Oceanogr. 38(8), 1741-1761.
- Pilskaln, C.H., Paduan, J.B., Chavez, F.P., Andereson, R.Y., Berelson, W.M., 1996. Carbon
 export and regeneration in the coastal upwelling system of Monterey Bay, central
 California. J. Mar. Res. 54, 1149-1178.
- Rea, D.K., Hovan, S.A., 1995. Grain size distribution and depositional processes of the mineral component of abyssal sediments: Lessons from the North Pacific. Paleoceanography. 10 (2), 251-258.
- Riebesell, U., Körtzinger, A., Oschlies, A., 2009. Sensitivities of marine carbon fluxes to ocean
 change. Proc. Natl. Acad. Sci. USA. 106(49), 20602–20609.
- 787 Schwing, F., O'Farreu, M., Steger, J. Baltz, K., 1996. Coastal upwelling indices, West Coast of
 788 North America, 1946-1955, US. Department of Commerce, NOAA Technical
 789 Memorandum NOAA-TM-NMFS-SWFS-231, La Jolla, California, 207 pp.
- Sigman, D.M., Boyle, E.A., 2000. Glacial/interglacial variations in atmospheric carbon dioxide.
 Nature. 407, 859-869.
- Small, L.F., Landry, M.R., Eppley, R.W., Azam, F., Carlucci, A.F., 1989. Role of plankton in
 the carbon and nitrogen bubgets of Santa Monica Basin, California. Mar. Ecol. Prog. Ser.
 56(1-2), 57-74.
- Sonnerup, R.E., Mecking,S., Bullister, J.L., 2013. Transit time distributions and oxygen utilization rates in the Northeast Pacific Ocean from chlorofluorocarbons and sulfur hexafluoride. Deep Sea Res. Part I. 72, 61-71.

- Steinberg, D.K., Van Mooy, B.A.S., Buesseler, K.O., Boyd, P.W., Kobari, T., Karl, D.M., 2008.
 Bacterial vs. zooplankton control of sinking particle flux in the ocean's twilight zone.
 Limnol. Oceanogr. 53(4), 1327-1338.
- Strub, P.T., Allen, J.S., Huyer, A., Smith, R.L., Beardsley, R.C., 1987. Seasonal cycles of
 currents, temperatures, winds, and sea level over the Northeast Pacific continental shelf:
 35°N to 48°N. J. Geophys. Res. 92(C2), 1507-1526.
- Stukel, M.R., Kahru, M., Benitez-Nelson, C.R., Décima, M., Goericke, R., Landry, M.R.,
 Ohman, M.D., 2015. Using Lagrangian-based process studies to test satellite algorithms
 of vertical carbon flux in the eastern North Pacific Ocean. J. Geophys. Res. 120(11),
 7208-7222.
- Stukel, M.R., Ohman, M.D., Benitez-Nelson, C.R., Landry, M.R., 2013. Contributions of
 mesozooplankton to vertical carbon export in a coastal upwelling system. Mar. Ecol.
 Prog. Ser. 491, 47-65.
- Suess, E., 1980. Particulate organic carbon flux in the oceans surface productivity and oxygen
 utilization. Nature. 288, 260-262.
- 813 Thunell, R., Benitez-Nelson, C., Varela, R., Astor, Y., Muller-Karger, F., 2007. Particulate
 814 organic fluxes along upwelling-dominated continental margins: rates and mechanisms
 815 Global Biogeochem. Cy. 21, 101029/102006GB002793.
- 816 Thunell, R.C., 1998. Particle fluxes in a coastal upwelling zone: sediment trap results from
 817 Santa Barbara Basin, California. Deep Sea Res. Part I. 45, 1863-1884.
- 818 Thunell, R.C., Varela, R., Llano, M., Collister, J., Muller-Karger, F., Bohrer, R., 2000. Organic
 819 carbon fluxes, degradation and accumulation in an anoxic basin: sediment trap results
 820 from the Cariaco Basin. Limnol. Oceanogr. 45(2), 300-308.
- 821 Tsunogai, S., Noriki, S., 1991. Particulate fluxes of carbonate and organic carbon in the ocean.
 822 Is the marine biological activity working as a sink of the atmospheric carbon? Tellus.
 823 43(2), 256-266.
- Turner, J.T., 2015. Zooplankton fecal pellets, marine snow, phytodetritus and the ocean's
 biological pump. Prog. Oceanogr. 130, 205-248.
- Van Mooy, B.A.S., Keil, R.G., Devol, A.H., 2002. Impact of suboxia on sinking particulate
 organic carbon: Enhanced carbon flux and preferential degradation of amino acids via
 denitrification. Geochim. Ac. 66(3), 457-465.
- Volk, T., Hoffert, M.I.. 1985. Ocean carbon pumps: analysis of relative strengths and
 efficiencies in ocean-driven atmospheric CO₂ changes, in: Sundquist, E.T., Broecker,
 W.S. (Eds.), The Carbon Cycle and Atmospheric CO₂: Natural variations Archaean to
 Present. Geophysical Monographs. American Geophysical Union, Washington, D.C. 32,
 pp. 99-110.
- Walsh, J.J., 1991. Importance of continental margins in the marine biogeochemical cycling of
 carbon and nitrogen. Nature. 350(6313), 53-55.
- Wong, C.S., Whitney, F.A., Crawford, D.W., Iseki, K., Matear, R.J., Johnson, W.K., Page, J.S.,
 Timothy, D., 1999. Seasonal and interannual variability in particle fluxes of carbon,
 nitrogen and silicon from time series of sediment traps at Ocean Station P, 1982-1993:
 relationship to changes in subarctic primary productivity. Deep Sea Res., Part II. 46(112735-2760.

842 FIGURE CAPTION

- Fig. 1. Chart (in m) of Monterey Bay and the location of M2, S1 and S2 moorings. The position
 at which Ekman transports were estimated is shown by a red square
- Fig. 2. Time series of (A) across shore Ekman transport at 36.5°N, 122.5°W (kg m⁻¹ s⁻¹);
 negative values indicate offshore transport associated with coastal upwelling. Time series for
- 848 the upper 200 m at the M2 site (shown in Fig. 1): (B) temperature (°C), (C) salinity, (D) nitrate 849 (μ M) and (E) primary production (mg C m⁻³ day⁻¹).
- Fig. 3. Time series of fluxes of (A) total mass, (B) C_{org}, (C) CaCO₃, (D) %C_{org} relative to total
 mass and C_{org}:N ratio (open circles) and (E) C_{org}: C_{inorg} ratio at 300 m.
- 853

850

- Fig. 4. Time series of fluxes of (A) total mass, (B) C_{org} and (C) CaCO₃, (D) %C_{org} relative to
 total mass and C_{org}:N ratio (open circles) and (E) C_{org}: C_{inorg} ratio at 1200 m.
- 856

Fig. 5. Annual cycle of (A) across shore (solid line) and alongshore (dashed line) Ekman
transport (kg m⁻¹ s⁻¹), (B) integrated primary production in the photic zone (mg C m⁻² day⁻¹), (C)
alongshore (solid line) and across shore (dashed line) currents at 300 m (cm s⁻¹); positive
alongshore (across shore) currents are directed toward 346°T (76°T). (D) temperature at 300 m
(°C) (E) alongshore (solid line) and across shore (dashed line) currents at 1200 m (cm s⁻¹) and

862 863

873

(F) temperature at 1200 m (°C).

Fig. 6. Seasonal averages for (A) Total mass, (B) C_{org} and (C) $CaCO_3$, (D) % C_{org} relative to total mass and C_{org} :N ratio (open circles) and (E) C_{org} : C_{inorg} ratio at 300 m and (F) Total mass, (G) C_{org} and (H) $CaCO_3$, (I) % C_{org} relative to total mass and C_{org} :N ratio (open circles) and (J) C_{org} : C_{inorg} ratio at 1200 m. EU = early upwelling, February to April, LU= late upwelling, May to July, OC= oceanic, August to October, and DV =Davidson season, November to January.

Fig. 7. Relationship between observed mooring tilt and current speed at 300 m at the S2
mooring. Grey dots are individual 15-minute observations and dark grey dots are means of tilt
observations for each 1 cm s⁻¹ increment of speed.

Fig. 8. Scatter plot of organic carbon fluxes at 300 m (mg C m⁻² day⁻¹) vs. integrated primary
production (mg C m⁻² day⁻¹) during the period of sediment collection (usually two weeks).

Fig. 9.Scatter plot of integrated primary production vs. Offshore Ekman transport (kg m⁻¹ s⁻¹).
Integrated primary production (mg C m⁻² day⁻¹) and offshore Ekman transport values for each
point correspond to the average of integrated primary production and across shore Ekman
transport during the period of sediment collection (usually two weeks). Dot color scale
represents the magnitude of organic carbon fluxes (mg C m⁻² day⁻¹) for each sediment trap
sample.

883 Fig. 10. Average C_{org} flux for each LU seasons (from May to July) during the seven study years.

884

885 Fig. 11, Seasonal one dimensional budget of C_{org} , mg m⁻² day⁻¹ for Monterey Bay. The brown 886 arrow represents the potential lateral supply of resuspended material. EU is early upwelling,

- 887 February to April, LU is late upwelling, May to July, OC is oceanic, August to October, and DV
- 888 is Davidson season, November to January.

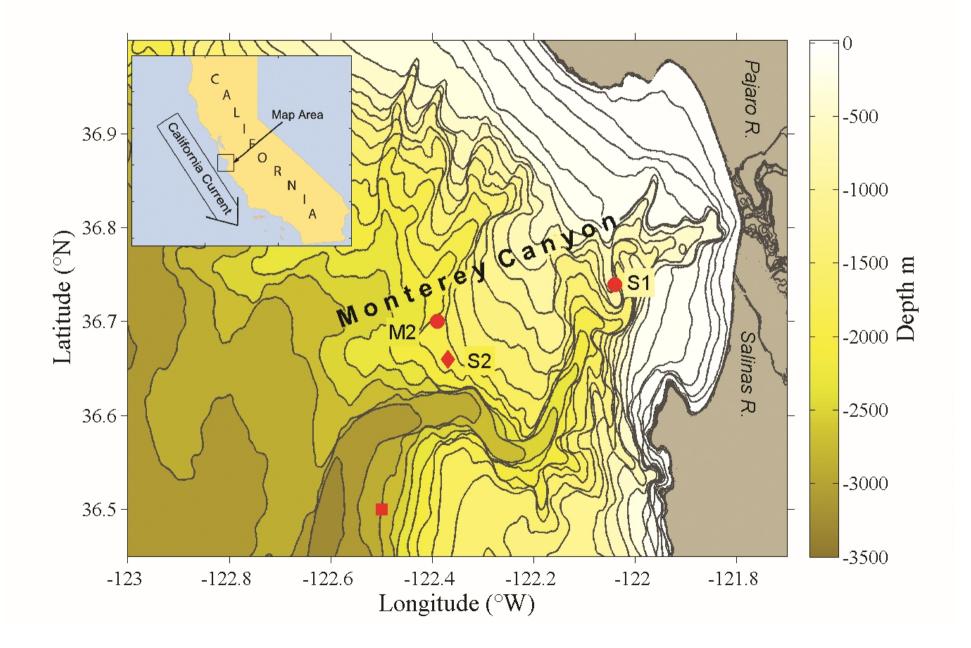
Deploy	Sampling period		Тгар Туре	e Interval	
1 2	Start	Finish	1 91		
	yy/mm/dd	yy/mm/dd			
300 m					
01	98/03/25	98/08/21	IRS	10 x 14, 1 x 9	
02	98/08/26	99/01/27	IRS	11 x 14	
03	99/02/10	99/07/14	IRS	11 x 14	
04	99/08/04	00/01/05	IRS	11 x 14 ¹	
05	00/02/09	00/07/12	IRS	11 x 14	
06	00/08/16	01/01/03	IRS	11 x 14 ²	
07	01/01/31	01/07/04	IRS	11 x 14 ²	
08	01/08/22	02/01/23	IRS	11 x 14	
09	02/02/08	02/07/10	IRS	10 x 14, 1 x 9	
10	02/09/04	03/02/05	IRS	11 x 14	
11	03/03/12	03/08/13	IRS	11 x 14	
12	03/09/10	04/02/11	IRS	11 x 14 ³	
13	04/03/17	04/08/18	IRS	11 x 14	
14	04/09/13	05/06/20	IRS	10 x 28	
1200 m					
01	98/03/25	98/08/21	Mark VI	10 x 14, 1 x 9	
02	98/08/26	99/01/13	Mark VI	10 x 14	
03	99/02/10	99/07/14	Mark VI	12 x 14 ⁴	
04	99/08/04	00/01/19	Mark VI	12 x 14	
05	00/02/09	00/07/12	Mark VI	11 x 14 ⁵	
06	00/08/02	01/01/17	Mark VI	12 x 14 ¹	
07	01/01/31	01/07/04	Mark VI	12 x 14 ⁶	
08	01/08/22	02/02/06	Mark VI	12 x 14	
09	02/02/08	02/08/07	Mark VI	12 x 14, 1 x 12	
10	02/09/04	03/03/05	Mark VI	13 x 14	
11	03/03/12	03/08/27	Mark VI	12 x 14	
12	03/09/10	04/03/10	Mark VI	13 x 14	
13	04/03/17	04/09/01	Mark VI	12 x 14	
14	04/09/13	05/06/20	Mark VI	10 x 28	

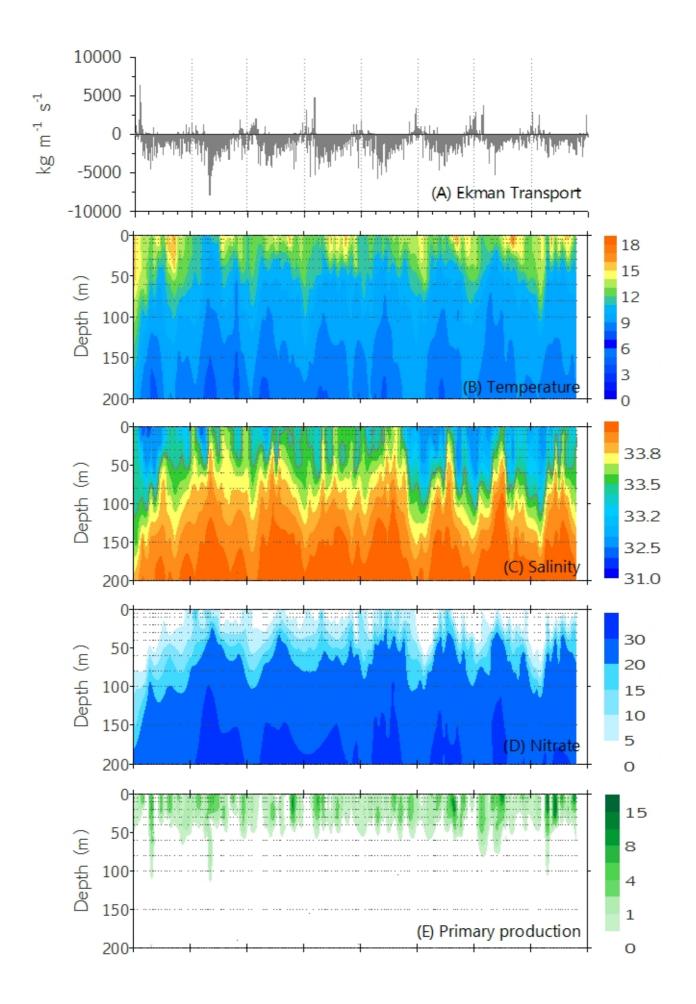
890 Table 1. Sediment trap deployment period, trap type, sampling interval and specific comments.

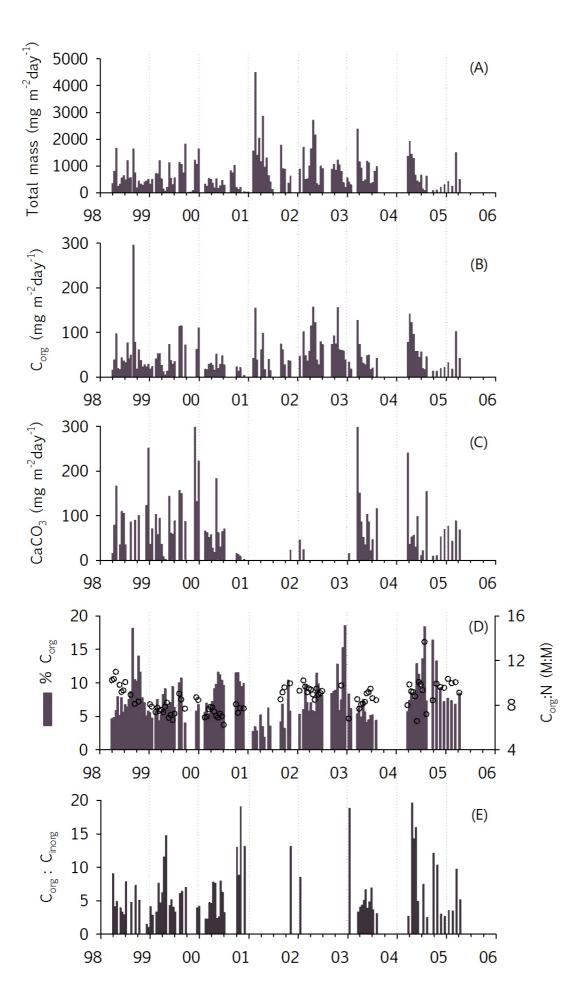
- 892 1 Insufficient material for the last 5 samples
- 893 2 Insufficient material for the last 4 samples
- 894 3 Program failed; missing all samples
- 895 4 Battery failed; missing all samples
- 896 5 Program failed; missing last 6 samples
- 897 6 Material clogged; missing last 8 samples

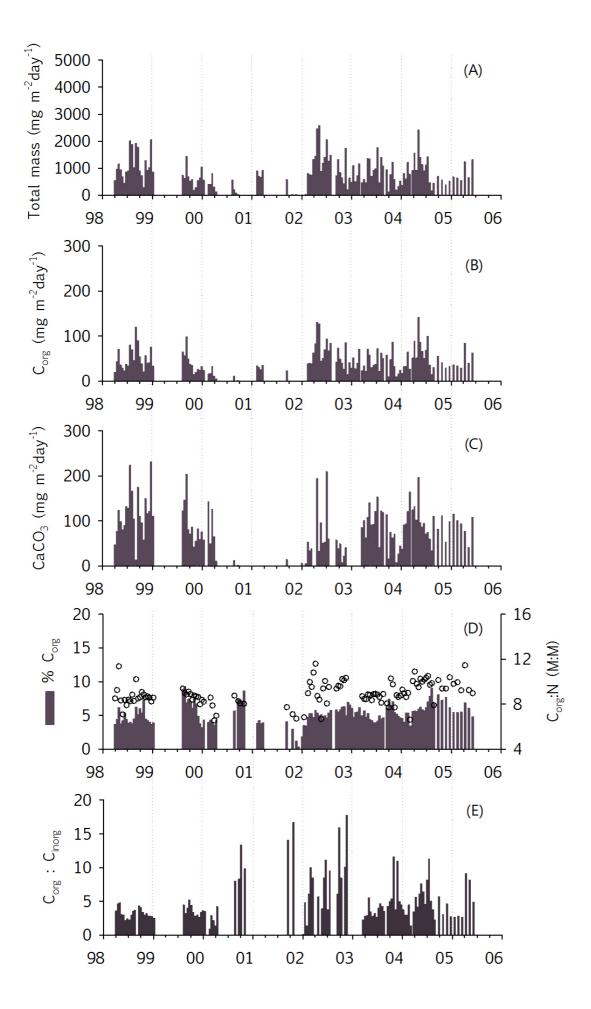
Table 2 Statistics of current speeds, cm s⁻¹ at the two sediment trap depths (300 m and 1200 m)
and frequency of time when mean currents > 15 cm s⁻¹. Seasons are defined as: EU is early
upwelling, February to April, LU is late upwelling, May to July, OC is oceanic, August to
October, and DV is Davidson season, November to January.

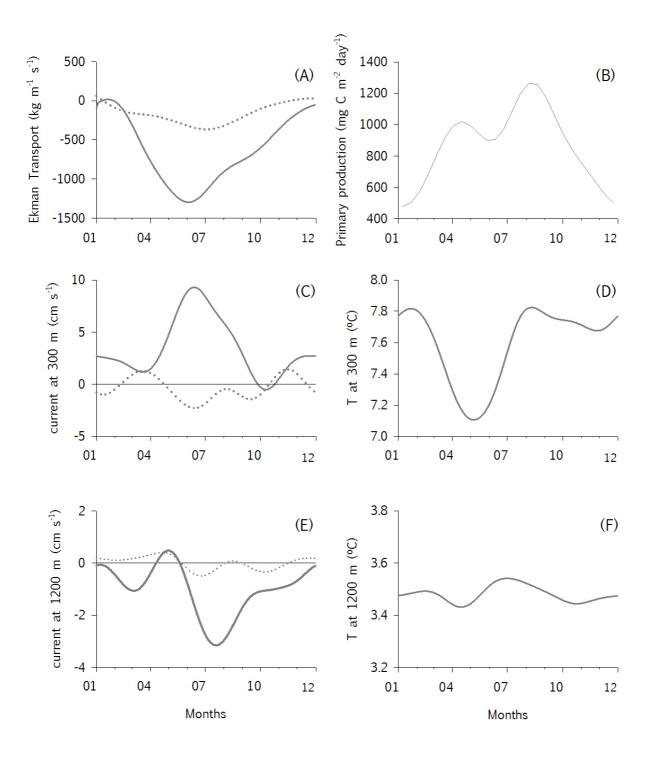
Year	Season	AVG 300 m	STD 300 m	v>15 cm s ⁻¹ 300 m	AVG 1200 m	STD 1200m
1998	EU	3.7	1.2	0%	1.75	0.86
1998	LU	12.4	4.0	33%	2.32	0.89
1998	OC	6.7	3.7	0%	2.16	1.57
1998	DV	7.0	5.1	0%	2.10	0.96
1999	EU	5.8	3.7	0%		
1999	LU	15.4	3.4	60%		
1999	OC	7.0	4.2	0%	3.16	1.88
1999	DV	7.2	2.7	0%	2.14	0.40
2000		~ ~	2.5	00/	1.04	0.62
2000	EU	5.5	3.5	0%	1.24	0.63
2000	LU	14.5	7.6	40%	1.07	1 41
2000	OC DV	13.3	4.0	40%	4.26	1.41
2000	DV	6.2	1.7	0%	3.48	1.21
2001	EU	6.7	4.6	0%	3.36	0.53
2001	LU	11.6	4.4	20%		
2001	OC	12.8	1.6	0%	2.48	0.74
2001	DV	7.8	3.4	0%	1.72	1.14
2002	EU	8.6	4.1	0%	1.90	1.33
2002	LU	13.2	5.2	20%	2.54	1.54
2002	OC	18.6	4.0	50%	3.70	2.10
2002	DV	8.5	2.8	0%	3.68	3.43
2003	EU	8.9	2.7	0%	4.02	3.43
2003	LU	13.3	3.9	33%	4.62	1.56
2003	OC	7.9	4.9	0%	2.82	1.40
2003	DV	6.0	2.3	0%	1.44	0.83
• • • • •				aa (
2004	EU	9.5	3.5	0%	3.73	2.54
2004	LU	11.3	6.2	29%	5.26	3.34
2004	OC	13.1	9.8	0%	3.58	1.25
2004	DV	6.5	2.8	0%	2.20	0.60
2005	EU	4.9	1.0	0%	1.94	1.80
2005	LU	13.5	1.0	0%	1.85	1.26
2000	LU	10.0	1.1	070	1.00	1.20

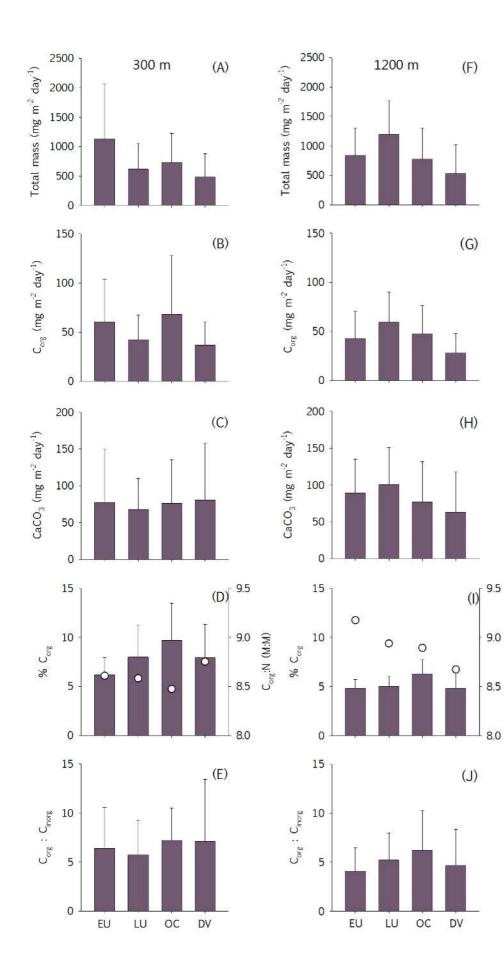




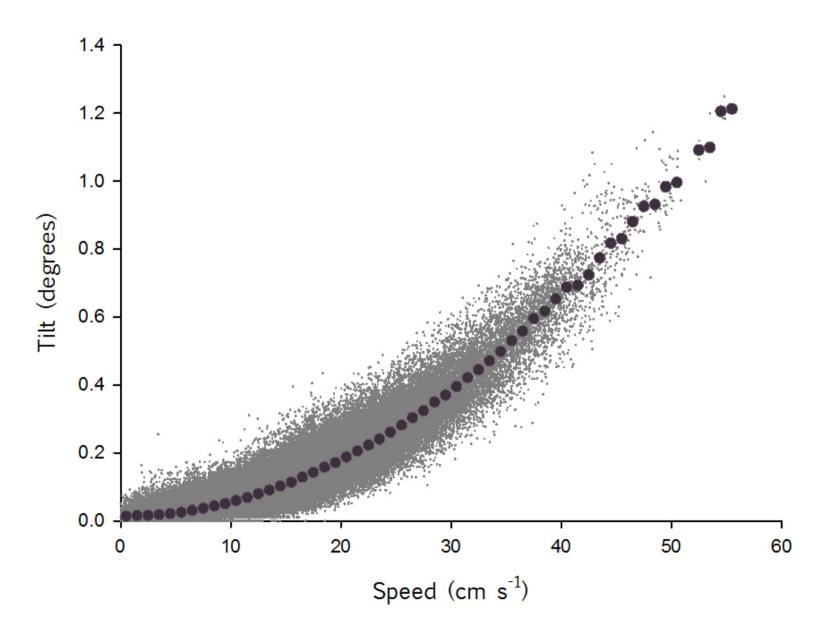


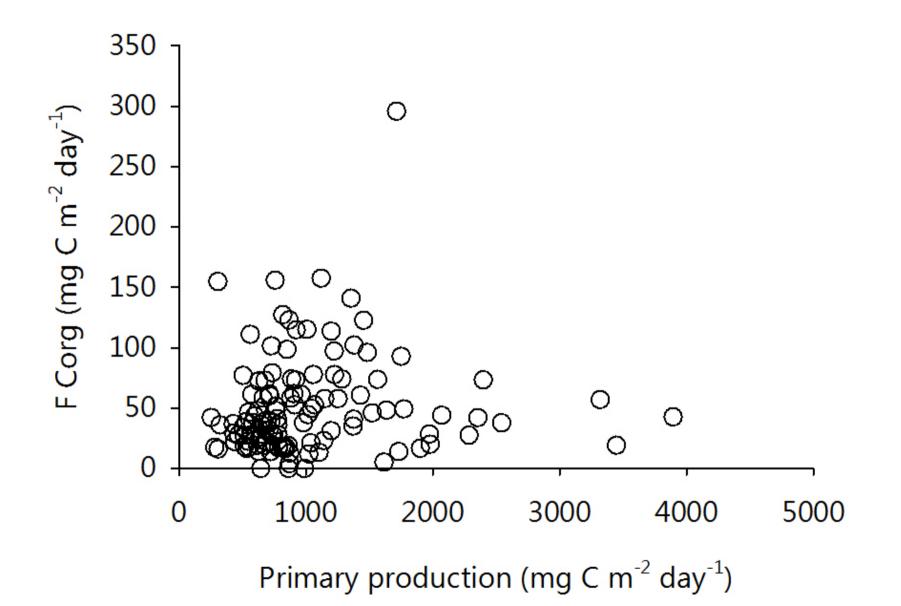


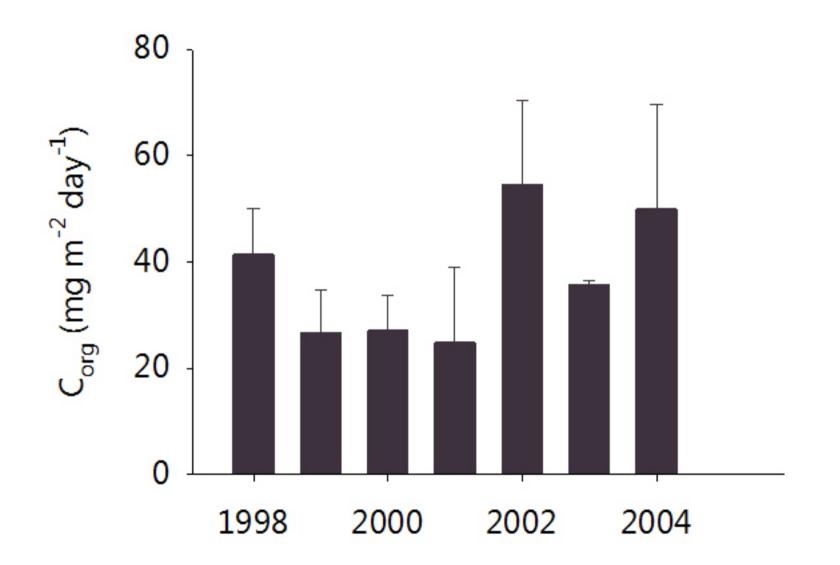


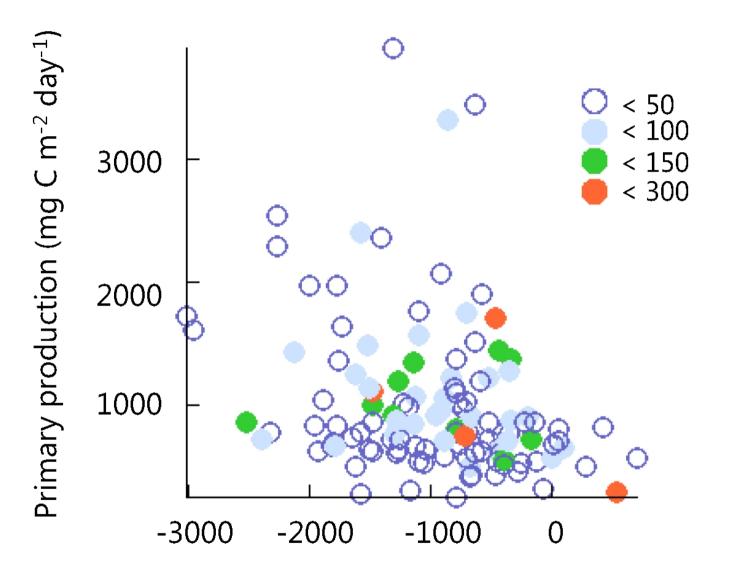


Corg:N (M:M)









Ekman Transport (kg m⁻¹ s⁻¹)

